IMPROVING THERMAL AND ELECTRICAL CONDUCTIVITY OF THERMOSETTING COMPOSITES WITH PLANT-BASED GRAPHENE

Daniel Mulqueen
Carbon Research and Development
Oleksandr G. Kravchenko
Old Dominion University

Abstract

Graphene has generated substantial interest as a filler due to its exceptional strength, flexibility, and conductivity but faces obstacles in supply and implementation. A renewable, plant-based graphene nanoparticle (pGNP) presents a more accessible filler with the same properties as mineral graphenes. In this study we examine the effects of pGNPs on a Bisphenol A resin at loadings from 1% to 25%, including the mechanical, thermal, and electrical properties. Preliminary results show pGNP addition improves mechanical properties at elevated temperatures, as well as dramatic increases in electrical and thermal conductivity, beginning at very low loadings. Methods for proper integration of pGNPs were considered to ensure even distribution, as agglomeration of particles can lead to decreases in material performance.

Background and Requirements

Plastic components offer several advantages for OEM parts manufacture, lighter weight, lower cost, and impact resistance, and plastic utilization is growing rapidly but traditional plastics are constrained by their thermal and electrical conductivity. Thermal conductivity in particular is seeing a growing demand as heat dissipation is of increasing concern for applications for miniaturized electronics to electric vehicle construction [1]. Lack of electrical conductivity still holds back use of reinforced thermosetting plastics in applications where conductivity is essential such as the aerospace industry [2]. Electrostatic painting systems are widely used in automotive coatings but have difficulty with plastic parts because of a lack of electrical conductivity [3]. Plastics are widely used for corrosion resistant tanks and piping, but static build up due to a lack of conductivity creates an explosions hazard [4]. Carbon nanomaterials, such as graphene, have exceptionally high carrier mobility which promises dramatic increases in electrical and thermal conductivity as well as benefits to the physical properties of the plastic parts [1-5].

Graphene nanoparticles (GNPs) have shown dramatic improvements of the thermal conductivity of epoxy composites, at both low and high loadings. When compared to traditional thermal interface fillers, a 5%(v/v) loading of graphene performs as well as 50-70% (v/v) loadings [6]. GNPs are superior to other carbon nanoparticles in this regard because their large surface area promotes efficient phonon transfer between the matrix and the nanoparticle [7]. GNPs have increased the decomposition temperatures of thermoplastic materials, but the effect is concentration dependent. At loadings up to 2% (w/w), GNPs retard the decomposition of the polymer, preventing structural breakdown. At higher loadings, GNPs increase the thermal conductivity of the composite, accelerating thermal decomposition [8]. Carbon nanomaterials, such as graphene, have tremendous potential in enhancing the interlaminar properties of the composite matrix when used as an interlaminar layer [9].

Likewise, graphene has shown a very low percolation threshold for increasing conductivity in polymers [8]. A 0.38% loading of isocyanate treated graphene oxide in polyamide lead to a

conductivity increase of eight orders of magnitude, along with increasing the strength of the film [10]. However, despite promising early results, graphene remains difficult to implement. Good graphene dispersion is essential, as well as good graphene/polymer interaction, however graphene loading and particle interaction can be too high, increasing agglomeration and reducing conductivity [11].

While graphene offers several benefits, it has yet to succeed widely in the marketplace for several reasons. Graphene has high levels of Van der Waals self-interaction, which can lead to aggregation and difficulty in dispersion and application. Graphene materials have also maintained a high cost, due to short supply of high-quality graphite precursors and difficulty on producing graphene nanoparticles. Further, graphene application can add cost and complexity to manufacturing. Hand rolling, or coating of graphene interlaminar layers can be time consuming and inconsistent. The use of interleaf layers adds complexity and mass beyond the low mass of interlaminar GNPs.

One GNP material, produced by the Carbon Research and Development Company (CRDC), is derived from biomass, offering lower costs and more available supply for an industrial additive. The CRDC process can utilize a wide range of lignocellulosic materials for pGNP production including timber and agricultural residues, as well as carbonaceous waste materials. Graphene production from mined graphite requires high purity, lump graphite with limited sources. In addition, there are several environmental concerns with mineral graphene production due to hazardous materials in wastewater [12]. Use of a biomass feedstock provides a renewable feedstock with opportunities for dramatic reductions in carbon emissions from shipping. The biomass derived pGNP contains a higher number of surface functional groups (SFGs) which increase interaction with simple solvents such as water, alcohol, and acetone resulting in a GNP which can be more easily utilized in simple applications such as spray coating. Further, epoxide functional groups offer opportunities for crosslinking in a thermoplastic matrix.

In this study, pGNPs will used to produce two composite materials. The first, representative of an industrial, high-performance composite, uses interlaminar layers of pGNPs which are spray-coated between layers of carbon fiber (CF)/bisphenol A epoxy prepreg. The pGNP/CF/epoxy system will be used to examine thermal and electrical conductivity of the complex composite. Increases in thermal and electrical conductivity are desirable, since they increase the range of applications that composite parts may be used in, as well as the range of conditions they will be effective under. Because of graphene's high surface area and low Van der Waal's interactions with other materials, there is concern that pGNP addition will affect bonding mechanics in the interlaminar region. The bonding strength of the cured resin in the composite will be measured using a T-Peel test. As a benchmark for pGNP/ bisphenol A epoxy interaction, a nanocomposite will be examined using pGNPs dispersed in an epoxy resin, examining curing mechanics as well as mechanical changes to the resin using hardness testing.

Experimental Methods

Materials

Epoxy resin used was Epon 828, manufactured by Hexion a bisphenol A/epichlorohydrin resin. The hardener selected was Epikure 3015, an aminodoamine with versatile cure characteristics. Carbon fiber/epoxy prepreg was purchased from Rock West composites. The unidirectional prepreg is composed of a Toray T800S fiber (63% w/w) in an intermediate modulus epoxy with a 135 ºC cure temperature and TG of 130 ± 10 °C.

Graphene nanoplatelets were provided by the Carbon Research and Development Company in a 7% w/w suspension with water. Platelet thickness range from 3-20 layers (1-6 nm) with a lateral size from 300-1000 nm. The nanoplatelets contain both epoxide and carboxyl functional groups, as well as some amorphous impurities. TEM imagining, as shown in Figure 1 shows stacked, multilayer graphene crystals with an interlaminar spacing of 0.345 nm. The interlaminar spacing is slightly larger than the 0.335 nm spacing typical of mineral graphene. The multi-crystal morphology is more similar to graphene crystals prepared by chemical vapor deposition than exfoliated mineral graphene.

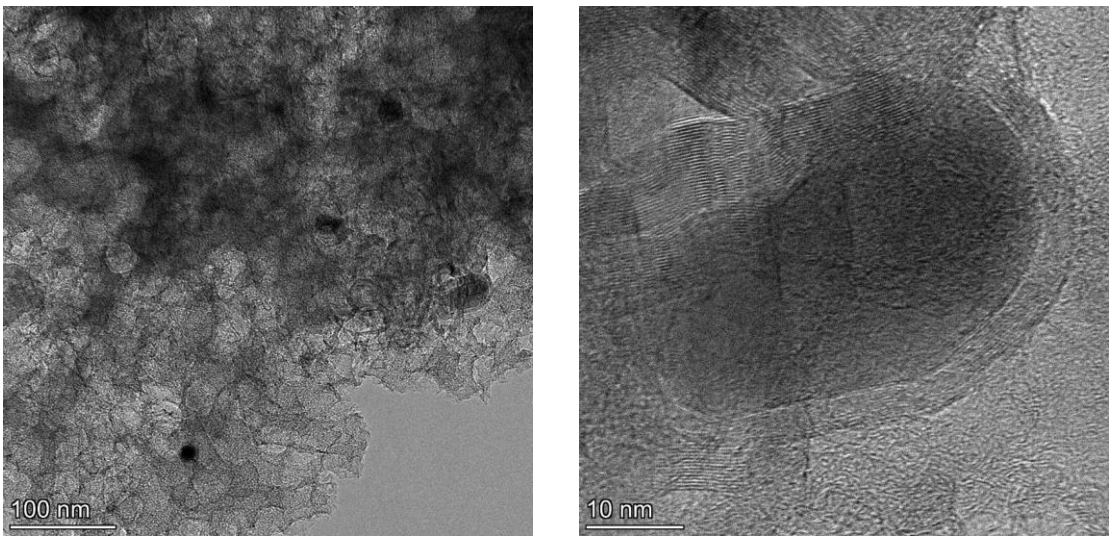

Figure 1: TEM scan of plant-based graphene nanoclusters. Interlaminar spacing is 0.345 nm.

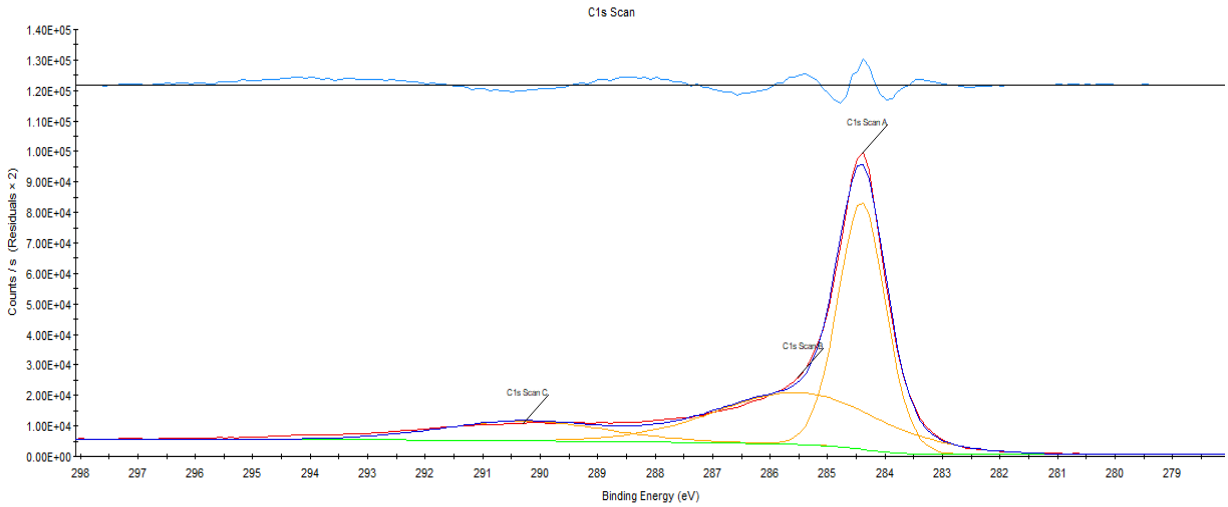

Figure 2: XPS analysis of surface scans show 49.82% sp2 (graphitic carbon), 36.34% C-O-C (graphene oxide/epoxide), and 13.83% O-C=O (carboxyl group).

Investigation of surface chemistry via X-ray photoelectron spectroscopy 87.0% C, 10.3% O, 1.4%N, and 1.3% other elements from wood ash. The structure of the carbon bonds on the

powder surface, as shown in Figure 2 showed 49.82 % sp2 graphitic/graphene bonding, 36.34% graphene-oxide/epoxide groups (C-O-C) and 13.83% carboxyl groups (O-C=O). Surface C:O ratio is 8.45:1, overall C:O ratio is >15:1, indicating that the majority of oxygen is located in surface functional groups.

pGNP dispersion in Resin

A pGNP/resin dispersion was formulated by heating the resin to reduce the viscosity, before adding pGNP and mixing in a benchtop high shear mixer (Pro Scientific PRO25D Homogenizer) for 30 minutes. The pGNP dispersion was mixed with hardener and cured following manufacturers guidelines.

Spray Formulation and Application

A GNP spray was formulated using a water/alcohol blend as the solvent. Water is a preferred choice over other solvents because of its ease of use and availability, as well as its lack of chemical interaction with the epoxy matrix. However, water has a much lower surface energy on the epoxy matrix as compared to isopropyl alcohol (Figure 3). The surface energy can be increased with the addition of surfactants and viscosity modifiers. A high surface energy results in a lower contact angle between a droplet and the surface and better wetting of the surface by the liquid. Addition of 42% isopropyl alcohol gives appropriate surface energy for even distribution.

A GNP spray solution was prepared by combining 210.56 g of graphene/water slurry with 1.8513 g of sodium dodecyl sulfate (SDS), 0.3846 g of carboxymethyl cellulose (CMC), and 171.3 g of 90% isopropyl alcohol and mixing until the SDS and CMC were thoroughly dissolved. The addition of SDS and CMC additives provide an improvement to the dispersion of graphene in the suspension, as well as drying and adhesion.

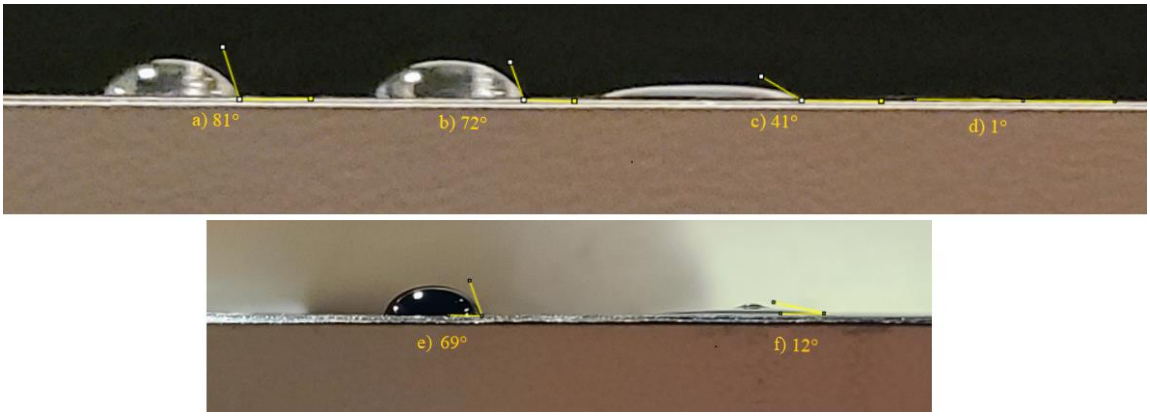

Figure 3: Contact angle measurements for: a) distilled water, b) DI with 1% CMC, c) DI with 1% SDS, d) 91% isopropyl alcohol, e) DI with pGNP/CMC/SLS, f) 42% isopropyl alcohol with pGNP/CMC/SLS.

Nanocomposite Preparation

CF/epoxy prepreg sheets were treated with pGNPs by spraying the prepared suspension through an airbrush onto the sheets by hand. In order to coat CF/epoxy prepreg sheets with pGNPs, an initial weight was taken before the sheets were hung vertically. The pGNP spray

suspension was applied using a pneumatic airbrush using even, overlapping passes. The prepreg is backed with paper on one side, the pGNP coating was applied to the non-backed side. Application rates were estimated by volumetric flow rate. As shown in Figure 4, sheets were hung vertically and sprayed evenly with the pGNP coating. Light coatings were used in order to ensure uniformity and to prevent beading on the prepreg surface. Coatings higher than 1.1 g/m^2 were sprayed in multiple coats. Sprayed sheets were weighed after sufficient drying to determine pGNP loading. The coated surface (Fig. 4 lower-right) is slightly less reflective than the uncoated surface (Fig. 4.lower-left).

Figure 4: Spray coating of CF/epoxy prepreg sheets.

Coating density can also be estimated using electrical resistance. Electrical conductivity across the surface of the dry, uncured ply was measured using an ohmmeter with a resistance of 17 Ω/mm, spray with the GNP solution at 1.7 g/m^2 reduced this to 1.8-3 Ω/mm. Further exploration of this is warranted.

Samples for curing kinetics and thermal conductivity were produced by stacking 168 2”x2” plies to a total thickness of 1”. Larger prepreg sheets were sprayed before cutting into 2”x2” plies and these plies were stacked with the pGNP sprayed surfaces laid against the untreated, paper backed surfaces with backing removed, providing interlaminar pGNP layers between each ply. A thermocouple was placed between plies 84 and 85, in the center of the sample to measure the heat reached internally.

T-peel samples were prepared within the guidelines of ASTM D1876. A test panel was prepared by joining two plies of prepreg, 125 mm wide and 305 mm long (in the fiber direction) with a 76mm Teflon insertion at one end and the pGNP coating between the plies. Test panels were cured under vacuum at 135 °C for 120 minutes before being cut to widths of ~20mm for testing.

Material Characterization of Fabricated Nanocomposites

Shore D Hardness

The harness of the cured pGNP/epoxy was measured with a Shore D durometer. The durometer was pressed against the sample until the value stabilized, and a reading was taken. Several values were taken and averaged. Shore D values (*S*) can be used as a first order approximation of the Youngs Modulus (*E*), as shown in Equation 1 [13],

$$S = 100 - \frac{20(-78.188 + \sqrt{6113.36 + 781.88E})}{E} \quad (1)$$

Given this relation, large changes in modulus will result in relatively small increases in hardness.

T-Peel Testing

T-Peel testing was performed as a measure of adhesive bonding force of the cured resin using an Ektron TS2000 universal testing apparatus which records the load/displacement history for each test. Tests were performed following the ASTM D1876 standard. The two plies of the composite are pulled under fixed displacement while recording load.

The energy release rate, G, is calculated by taking the average of the force applied after initial crack propagation (F), dividing by the sample width (b), and multiplying by a factor for the T-peel angle (90º) as shown in Equation 2

$$G = \frac{2F}{b} \quad (2)$$

Curing and Thermal Conductivity

To observe the effects of thermal conductivity on the curing of large composite members, composite samples were produced by stacking 168 2”x2” plies to a total thickness of 1”. A thermocouple was placed in the center of the sample to measure the heat reached internally. These samples were cured under vacuum on a flat mold in a convection oven, without additional pressure and were heated at a rate of 2.8 °C/min to 135 °C for 120 minutes, while internal temperatures were logged.

Thermal conductivity was measured by placing the composite sample in series with a 2” 304 stainless steel cube in between two plates of a heated press. As shown in Figure 5, the lower plate, in contact with the steel cube was heated to 150ºC, while the upper plate was held static at 20 ºC. Refractory material prevents heat transfer from radiant and convective means, while a nominal pressure ensures good contact between all faces. Thermocouples on the contact faces between the samples and plates provided temperature and heat flux information used to calculate the thermal conductivity of the sample.

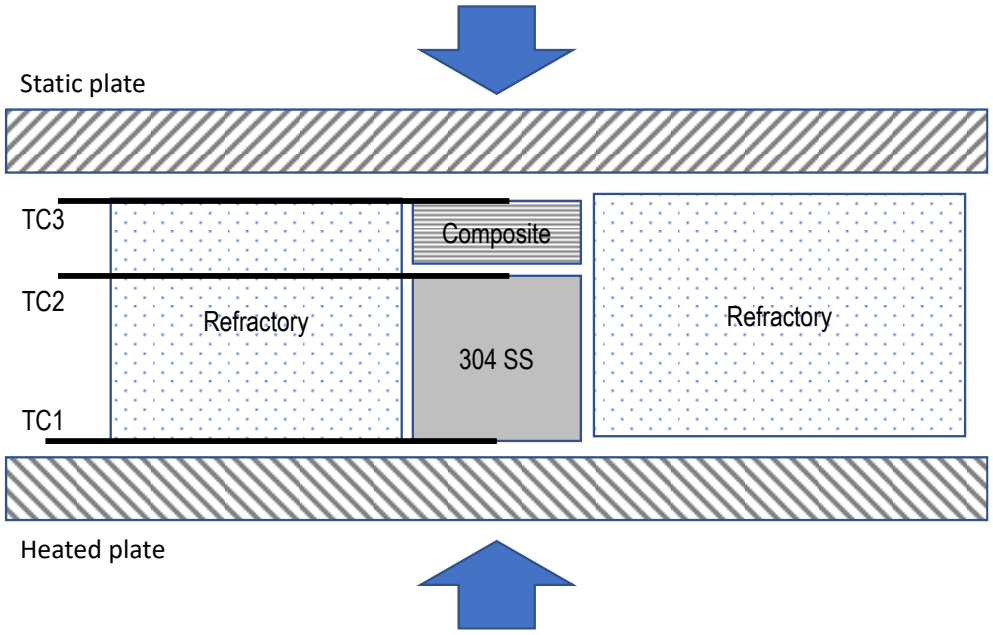

Figure 5: A profile of the thermal conductivity test setup.

Thermal conductivity for the sample was calculated by measuring the heat flux, Q, through the steel cube according to the heat flux equation;

$$Q = \frac{-k_s * A * \Delta T_s}{x_s} \tag{3}$$

where ΔT_s is the temperature differential across the cube, A is the area of the cube, x_s is the thickness, and k_s is the thermal conductivity of the stainless steel. Because the heat flux through the cube and the sample is the same, we can derive an equation for the thermal conductivity of the sample, k_u based on the temperature differentials across the sample and the steel cube:

$$k_u = \frac{x_u k_s \Delta T_s}{x_s \Delta T_u} \tag{4}$$

where ΔT_u is the temperature differential across the sample and x_u is the thickness of the sample.

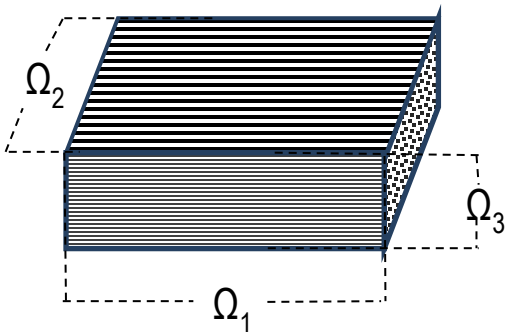

Figure 6: Electrical resistance was measured along the fiber direction, perpendicular to the fiber direction, and across the thickness of the composite.

Electrical resistance was measured using a Cen-Tech p37772 digital multimeter across the sample in the fiber direction (Ω_1), perpendicular to the fiber direction (Ω_2), and in the out-of-plane direction across the composite thickness (Ω_3) ad shown if Figure 6.

Results and Discussion

Modified Properties of Epoxy Nanocomposite

The pGNP shows a clear chemical interaction with the epoxy system. There is no interaction with Epon 828 after pGNPs are dispersed and the mixture is stable for up to 120 hours, but at pGNP loadings over 1 phr, the resin heats noticeably and foams when mixed with the 3015 hardener. A 25 phr pGNP loading resulted in internal temperatures of over 75 C after one hour of curing with no external heating, along with substantial hardening. This is noteworthy, considering the 808/3015 system has a cure time of 16 hours under ambient conditions.

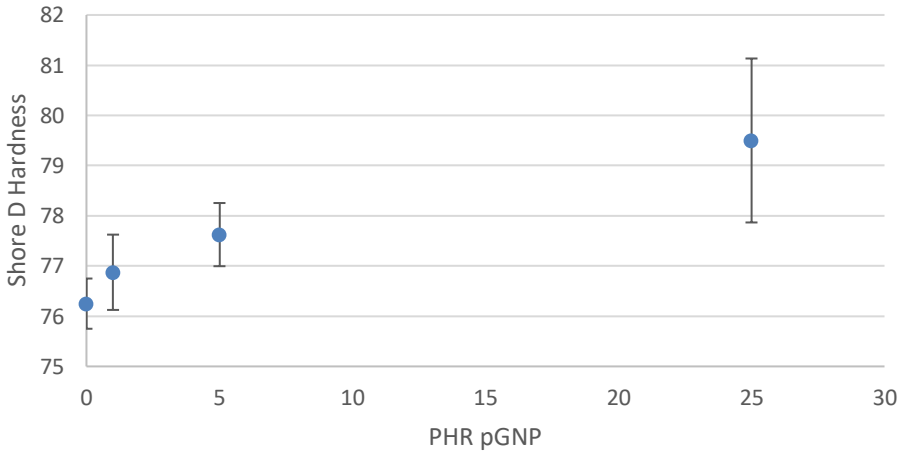

Figure 7: The increase in Shore D hardness of the cured 828 resin with increasing pGNP content.

Shore D hardness increases with pGNP content, as shown in Figure 7. The overall increase in hardness appears small, with increases of 0.82% at 1 phr and 4.26% at 25 phr, but the relation to Young's Modulus as shown in Equation 1 corelates significant increases in strength to moderate increases in hardness. There is a diminishing utility for loading at higher levels, with the greatest relative increase in hardness at 1 phr of pGNPs.

T-Peel Testing of Cured Unidirectional Composite with pGNP

T-Peel tests were performed at pGNP loadings of 0, 1.7, 3.4, 4.22, and 8.28 g/m^2, as shown in Figure 8. Results are presented in Table II. These loadings correspond to resin loadings of 0%, 2.0%, 3.9%, 4.9%, and 9.6%. The average energy release rate, which is an indicator of the adhesive bond, is 1822 J/m2, with a variance of 2.8%. Even at high loadings, the bond strength of the resin was not affected by the pGNP addition. A representative T-Peel load-displacement curve is included in Figure 9, showing progressive loading until initial crack propagation and the subsequent load as the plies are separated.

Figure 8: T-Peel testing of pGNP/CF/epoxy composites.

Table I: Adhesive bonding force of pGNP enhanced resin measured by T-Peel test

pGNP Loading (g/m2)	G (J/m2)	% Variance
0	1855	10%
1.7	1798	8%
3.4	1790	18%
4.22	1760	2%
8.28	1905	2%

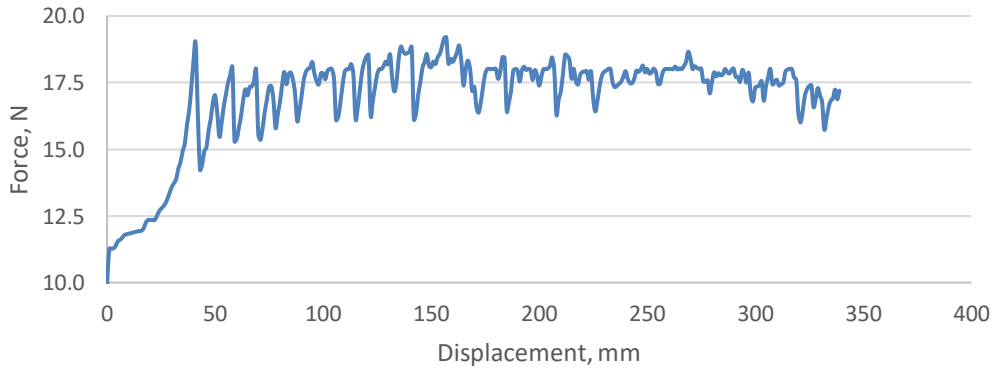

Figure 9: The load-displacement curve of a T-Peel test on an 8.28 g/m2 loaded pGNP composite.

The reactive effect on curing was also observed with the Rock West prepreg system. Increased pGNP correlated with an increase in the peak temperature reached during curing. Figure 10 shows the exothermic portion of the cure cycle for pGNP loaded composites. A negligible difference in internal curing temperature was observed at 1.1 g/m^2 loading, after which the internal temperature rose substantially with increased loadings to a total of 9.3 °C at 4.2 g/m^2. There is also a slight delaying of the exothermic cycle with increased loading. The increase in temperature may be due to chemical interaction with the resin, due to microscopic foaming reducing heat transfer, or a combination thereof. Further investigation will be required to understand the changes to curing dynamics.

Table II: Maximum curing temperature of pGNP treated composites

Coating density g/m^2	Resin mass fraction %	Maximum temperature °C
0	0.0%	185.84
1.1	1.3%	186.35
2.8	3.3%	191.36
4.2	4.9%	195.16

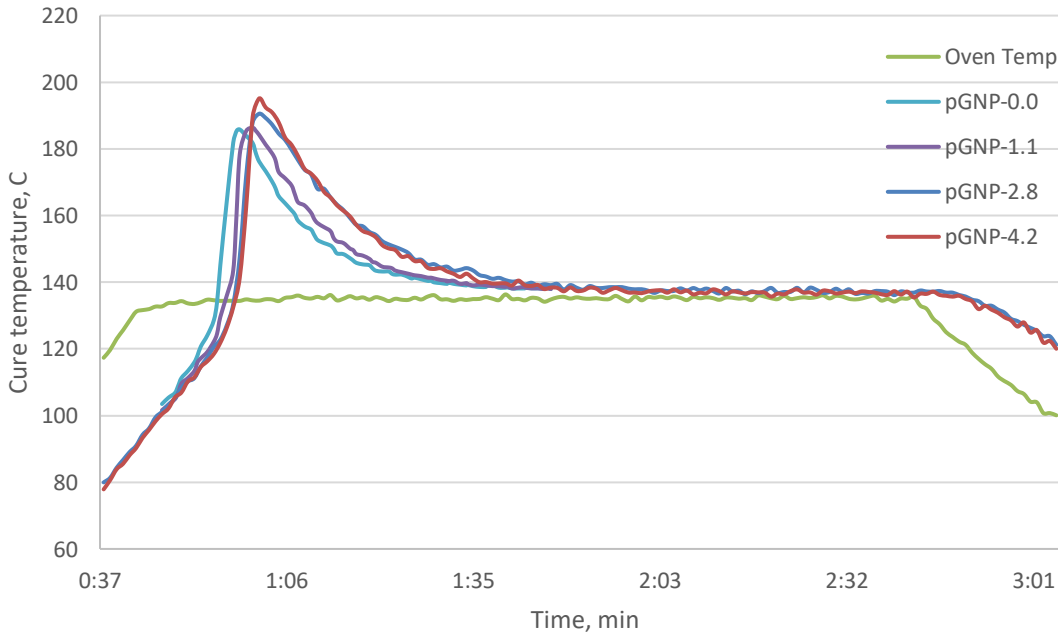

Figure 10: Exotherm profiles of curing composite blocks at various graphene loadings, with the oven air temp as a reference.

Thermal conductivity in a composite sample with a 1.1 g/m^2 spray loading increased thermal

conductivity in the 3 direction by 45%. Electrical conductivity was increased, but the increase varied depending on the axis of measurement, as shown in Table III below.

Table III: Resistance of pGNP treated composites

Orientation	Untreated	1.1 g/m^2	2.8 g/m^2	4.2 g/m^2
1	5.3 Ω/cm	2.1 Ω/cm	1.7 Ω/cm	1.4 Ω/cm
2	23.0 Ω/cm	8.0 Ω/cm	9.3 Ω/cm	7.7 Ω/cm
3	92.1 Ω/cm	47.4 Ω/cm	34.8 Ω/cm	34.8 Ω/cm

As with hardness, there is a diminishing return in conductivity after 1.1 g/m^2, with plateauing values at 2.8 and 4.2 g/m^2, showing that the percolation threshold has been reached. The directional relation to electrical conductivity is intuitive, given the application of pGNPs as an interlaminar layer. Layers of graphene contribute more to electrical conductivity in plane than they do out of plane.

Summary and Next Steps

Graphene offers substantial benefits to thermoplastic systems, including increases to thermal and electrical conductivity at very low loadings but understanding the interactions between the specific GNPs used and the material system is essential [11]. Previous work has shown that dispersion of GNPs is essential to strong performance, and we have shown that both dispersion into resin prior to curing and spray application onto prepreg sheets are successful at achieving good material performance. Examination of composite materials with microscopy will confirm pGNP distribution. The consistent G value of the cured resin shown that there is no degradation in the adhesive strength, even at very high pGNP loading.

pGNP interlaminar addition increased the thermal and electrical conductivity of CF/epoxy samples at loadings as low as 1.1 g/m^2. The directional dependance on electrical conductivity offers potential to construct parts which are conductive in one direction more so than in others. Thermal conductivity was only measured across the composite thickness because of limitations in the test setup, but similar directionality of thermal conductivity will be investigated. In every measured property, there was marginal utility of increased pGNP loading at higher levels. Future work will focus on loadings below 1%.

Direct suspension of pGNPs in resin offers a simple and effective means of utilizing graphene in composite systems. Interlaminar spray coatings offers a scalable means of pGNP application that can deliver unique properties to manufactured parts. The increases in Shore D hardness indicate that increases in resin modulus should be investigated. Printing of pGNPs onto prepreg sheets could allow for engineering paths of thermal and electrical conductivity. Direct measure of electrical conductivity has the potential to provide in situ information on pGNP coating thickness and distribution. Future work will focus on developing this method of measurement.

In both applications, there was an interaction between the pGNP particles and the curing resin. This interaction warrants further study and may be able to be utilized to improve pGNP/epoxy material properties. Epoxide and carboxyl functional groups on the pGNP surface are likely involved. Improvements to SFG utilization and curing dynamics present opportunities for

improvements to strength and conductivity.

Fillers are an often-overlooked element in green material design. Renewable pGNPs offer an effective, plant-based alternative to other carbon nanoparticles, with a greater potential supply and reduced environmental impact. Further development will expand on the benefits and applications of sustainable, plant-based carbon nanoparticles in plastic composite materials.

Acknowledgements

Dali Quan at University of Kentucky, Electron Microscopy Center for providing TEM and XPS data.

Bibliography

1. Sherman, L. M., "A Bright Future for Thermally Conductive Plastics," Plastics Technology July 2019, https://www.ptonline.com/articles/a-bright-future-for-thermally-conductive-plastics
2. Liu, J., Y. Li, D. Xiang, C. Zhao, B. Wang, H. Li, "Enhanced electrical conductivity and interlaminar fracture toughness of CF/EP composites via interleaving conductive thermoplastic films," Advanced Composite Materials 28, 2021, (17-37)
3. "Graphene nanotubes in plastics are the basis for cars of the future" August, 2020, https://www.plastech.biz/en/news/Graphene-nanotubes-in-plastics-are-the-basis-for-cars-of-the-15628
4. Clark, R. "Real world graphene: Industrial applications for the 21st century," Graphite Supply Chain 2017, http://imformed.com/wp-content/uploads/2017/11/Clark-Graphite-Supply-Chain-2017.pdf
5. Geim, A. K. & K. S. Novoselov, "The Rise of Graphene," Nature Materials 6, 2007, 183–191
6. Yu, A., P. Ramesh, M.E. Itkis, E. Bekyarova, R.C. Haddon, "Graphite Nanoplatelet−Epoxy Composite Thermal Interface Materials," J. Phys. Chem. C, 111 (21), 2007, 7565–7569
7. Teng, C., C. M. Ma, C. Lu, S. Yang, S. Lee, M. Hsiao, M. Yen, K. Chiou, T. Lee, "Thermal conductivity and structure of non-covalent functionalized graphene/epoxy composites," Carbon, 49, 2011, 5107-5116
8. Liu, H., M. Dong, W. Huang, J. Gao, K. Dai, J. Guo, G. Zheng, C. Liu, C. Shena, Z. Guo, "Lightweight conductive graphene/thermoplastic polyurethane foams with ultrahigh compressibility for piezoresistive sensing," J. Mater. Chem. C, 73, 2017, 1-240
9. Park, Y.T., Y. Qian, C. Chan, T. Suh, M.G. Nejhad, C.W. Macosko, A. Stein, "Epoxy toughening with low graphene loading," Adv. Funct. Mater. 25 (4), 2015, 575–585
10. Luong, N.D., U. Hippi, J.T. Korhonen,A.J. Soininen, et al. "Enhanced mechanical and electrical properties of polyimide film by graphene sheets via in situ polymerization," Polymer, 52, 2011, 5237-42.
11. Gong, G. "Literature study of graphene modified polymeric composites," Sio Grafen January 2018
12. Jara, A. D., A. Betemariam, G. Woldetinsae, J. Y. Kim, "Purification, application and current market trend of natural graphite: A review," International Journal of Mining Science and Technology, 29 (5), 2019, 671-689
13. Qi, H. J., K. Joyce, M.C. Boyce, "Durometer hardness and the stress-strain behavior of elastomeric materials," Rubber Chemistry and Technology, 76 (2), 2003, 419–435.